Measurement of radiation asymmetries during disruption mitigation at JET

P. Drewelow[1], U. Kruezi[2], H.R.Koslowski[3], M.Lehnen[4], G.F. Matthews[2] and JET Contributors*

EUROfusion Consortium, JET, Culham Science Centre, Abingdon, OX14 3DB, UK

[1] *Max-Planck Institute für Plasma Physik, Euratom Association, 17491 Greifswald, Germany*

[2] *CCFE, Culham Sience Centre, Abingdon OX14 3DB, UK*

[3] *Forschungszentrum Jülich GmbH, 52425 Jülich, Germany*

[4] *ITER Organization, Route de Vinon-sur-Verdon - CS 90 046,13067 St Paul Lez Durance Cedex, France*

Disruptions, the accidental loss of current and confined energy in Tokamak plasmas can cause damage to the in-vessel components and vital plant and support structures. Thus, the ability to predict, to avoid and if inevitable to mitigate this harm is crucial for existing fusion experiments and for future fusion reactors like ITER. Massive Gas Injection (MGI) is a possible approach to be used as a disruption mitigation system (DMS) enabling radiative dissipation of the stored energy. However, toroidal asymmetries in the radiation can diminish the energy dissipation and it is expected that in the case of ITER such asymmetries in the radiation could cause melting.

Setup at JET

At JET, the Tokamak experiment closest to ITER in terms of operating parameters and size, a DMS based on two fast disruption mitigation valves (DMV) has been established and is routinely used in close loop operation [1]. The toroidal location of these valves and their approximated injection trajectories are shown in figure 1 (DMV1: orange, DMV2: green). In order to study the mitigation efficiency at JET, bolometric measurements are used to assess the radiation level and distribution. The overview bolometer KB5 consisting of two cameras (red and blue in figure 2) allows a reconstruction of the poloidal radiation pattern by tomography. However, this analysis of the vertical and horizontal bolometer data assumes toroidal symmetry of the radiation and is known to produce artefacts in case this assumption does not hold. Thus, a set of

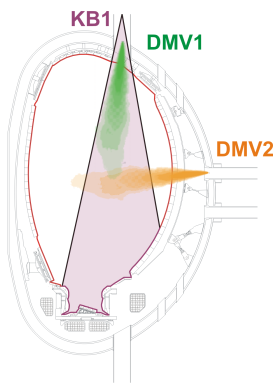

Figure 1: *Poloidal cross section JET torus*

*See the Appendix of F. Romanelli et al., Proceedings of the 25th IAEA Fusion Energy Conference 2014, Saint Petersburg, Russia four single channel bolometers (KB1) at different toroidal positions with an equivalent field of view (FOV) was recently re-installed (purple in figure 1 and 2).

Experiments and data analysis strategy

Due to limitations in the data acquisition of the single channel bolometer KB1, a mitigated disruption was repeated four times and the toroidal radiation distribution measured with each of the four bolometers consecutively. The main plasma parameters prior to the disruption (central density $n_e = 6 \cdot 10^{19} m^{-3}$ and temperature $T_e = 1.8$keV, plasma current $I_p = 1.5$MA, total radiation $P_{rad} = 3$MW and input heating power $P_{NBI} = 14$MW) are all comparable during the pulse. Tomographic reconstructions show a similar poloidal radiation pattern in the pre-disruption plasma. All time vectors are corrected by the time t_{DMV} when the DMV puff reaches the plasma. The DMV delivered 10bar l of a gas mixture of 10% Argon and 90% Deuterium.

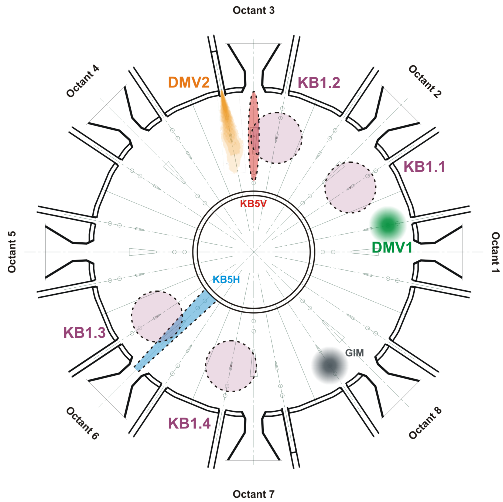

Figure 2: *Horizontal overview of measurement setup at JET*

The radiated power $P_{\mathrm{rad,\,i}}$ measured by each KB1 bolometer i is derived using the bolometer equation

$$P_{\mathrm{rad,i}} = \frac{\tau_{\mathrm{i}} G_{\mathrm{i}}}{S_{\mathrm{i}} g} \times \left(\frac{dU_{\mathrm{i}}}{dt} + \frac{U_{\mathrm{i}}}{\tau_{\mathrm{i}}} \right) \tag{1}$$

with the voltage signal of KB1 U_{i}, the cooling time of the detector foil τ_{i}, the amplification factor of the data acquisition g, the detector sensitivity S_{i} and the etendue of the field of view G_{i}. Most of these parameters are known, except for S_{i} and G_{i}. They are derived using a cross calibration to the total power $P_{\mathrm{rad,tot}}$ measured by the vertical camera of the KB5 bolometer in octant 3 during a phase of complete toroidal symmetry of the plasma (limiter start-up or a divertor fuelled symmetrically heated phase).

The cross calibration $P_{\mathrm{rad,o}} = k_{\mathrm{geo}} \times P_{\mathrm{rad,i}} = \frac{1}{8} P_{\mathrm{rad,tot}}$ can be used to derive an estimate for the radiation $P_{\mathrm{rad,o}}$ in each octant o, assuming a constant geometry factor k_{geo} that represents the ratio between the radiation within the FOV of KB1 and that within the total volume of one octant. This assumption may not hold for a plasma with asymmetry even within one octant or when a large fraction of the radiation is not within the poloidal FOV of KB1 (e.g. torus inboard side, see figure 1). Dividing $\frac{\max[P_{\mathrm{rad,o}}]}{\mathrm{mean}[P_{\mathrm{rad,o}}]} = f_{\mathrm{TRPF}}$ results in the toroidal radiation peaking factor which is unaffected by the geometric factors. In the following, an average $\langle f_{\mathrm{TRPF}} \rangle$ is shown that

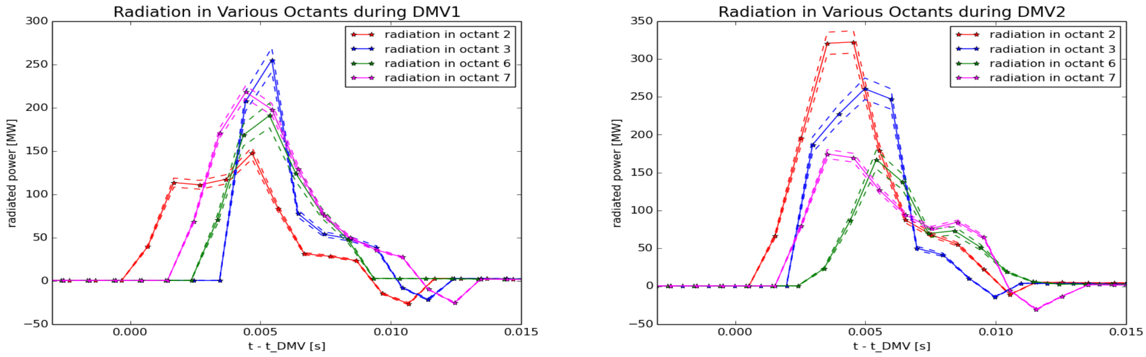

(a) (b)

Figure 3: *Radiated power during the application of (a): DMV 1 (vertical in octant 3) and (b): DMV 2 (horizontal in octant 6)*

is derived from the integral radiated energy.

The toroidal asymmetry measurement was validated with the integrated radiated energy during a pulse fuelled by a Gas Inlet Module (GIM) in octant 8 (see figure 4). The peaking at octant 7 agrees with asymmetry induced artefacts observed in the tomographic reconstruction.

Radiation characteristics during disruption mitigation

Using the vertical injection valve in octant 1 (DMV1) during a disruption resulted in a radiation that was detectable in the octant order: 2, 7, 6 and 3 (see figure 3 (a)). Since KB1.3 ($\Delta\varphi = -157.5°$) is reached before KB1.2 ($\Delta\varphi = +67.5°$), the clockwise expansion of the radiation cloud seems about three times as fast as in anti-clockwise direction. When integrating the radiation during the disruption (neglecting the negative drop in figure 3 (a)), the main radiation was emitted in octant 7 rather than in 2 (see figure 4, green line). This indicates a preferred clockwise gas or impurity transport that leads to an average toroidal peaking of $\langle f_{\text{TRPF}} \rangle \approx 1.3$ in octant 7. Mitigating the disruption with a horizontal gas injection at octant 3 (DMV2), the radiation occurs in the order octant 2, 7, 3 and 6 (see figure 3 (b)). Due to its proximity, the radiation signal would be expected first in octant 3 (see figure 2). It is possible that it only seems delayed after the octant 2 radiation because

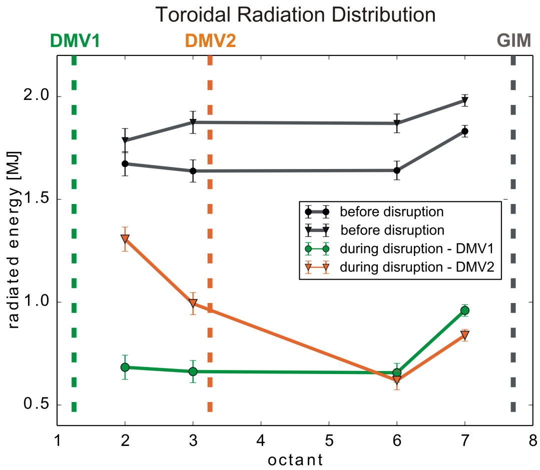

Figure 4: *Toroidal distribution of radiated energy before and during the disruption mitigated by different DMV1 and DMV2*

poloidally the radiation is limited to the blind angle of KB1.2 (see figure 1) in the first phase of the disruption. The integral radiation during the disruption peaks at octant 2 with $\langle f_{\mathrm{TRPF}} \rangle \approx 1.4$. Apart from the slightly higher $\langle f_{\mathrm{TRPF}} \rangle$ value it should also be noted that the radiation peak extends further around the torus with horizontal injection (ca. over octant 7-8-1-2-3), while it only covers up to three octants (7-8-1) during the vertical gas injection (see figure 4).

Conclusion

Measuring the toroidal radiation distribution with a set of four toroidally distributed bolometers revealed differences in the radiation peaking during a disruption mitigated by horizontal or vertical massive gas injection. Both injections resulted in a similar peaking factor (vertically 1.3, horizontally 1.4). The peak location seems shifted in both cases by $\Delta\varphi_{\mathrm{peak}} \approx 20^\circ$ to $\Delta\varphi_{\mathrm{peak}} \approx 50^\circ$ toroidally. This stands in contrast to simulations at DIII-D [3], predicting the radiation peak on the opposite torus side due to a gas puff induced $1/1$ MHD mode. The average radiated energy peaking is also of a lower level than the previously measured transient peaking factor in the pre-thermal-quench phase of 8 [2] indicating that the thermal-quench radiation compensates by far the initial radiation located at the gas injection point. The injection methods differ in the toroidal width of the total radiated energy peak. Vertical injection confines the peaking to maximal three octants, while horizontal injection causes a broad peak extending over at least 5 octants. This difference might be related to a wider gas diffusion in the larger volume outside the plasma that is available at the horizontal injection point.

Future work will focus on a more systematic investigation into the interaction of the gas puff with pre-existing MHD modes or plasma rotations and on the further analysis of the time resolved peaking in different phases of the disruption.

Acknowledgement

This work has been carried out within the framework of the Contract for the Operation of the JET Facilities and has received funding from the European Union's Horizon 2020 research and innovation programme. The views and opinions expressed in this paper do not necessarily reflect those of the European Commission or the ITER Organization.

References

[1] U. Kruezi et al, Proceedings of 28th SOFT, EFD-C(14)05/22 Dia ref. CPS14.691 (2014)

[2] M. Lehnen et al, Nuclear Fusion **51**, 123010 (2011)

[3] Izzo V.A., Physics of Plasmas **20**, 056107 (2013)